THE JOURNAL OF PHYSICAL CHEMISTRY B

Article

pubs.acs.org/JPCB

Distribution of Neutral Lipids in the Lipid Droplet Core

Vitaly V. Chaban* and Himanshu Khandelia*

MEMPHYS − Center for Biomembrane Physics, Syddansk Universitet, Odense M., 5230, Denmark

ABSTRACT: Cholesteryl esters (CEs) are a form of cholesterol (CHOL) storage in the living cells, as opposed to free CHOL. CEs are major constituents of low density lipoprotein particles. Therefore, CEs are implicated in provoking atherosclerosis. Arranged into cytoplasmic lipid droplets (LDs), CEs are stored intracellularly. They can also be transported extracellularly by means of lipoproteins. In this work, large-scale molecular dynamics (MD) simulations are used to characterize the molecular structure of LDs containing various fractions (10−50 mol %) of cholesteryl oleate (CO) with respect to triolein (TO) fraction. The simulated LDs were covered by a phospholipid monolayer formed by a mixture of 1-palmitoyl-2-oleoylphosphatidylcholine, POPC (75 mol %), and 1-palmitoyl-2-oleoyl-*sn*-glycero-3-phosphoethanolamine, POPE (25 mol %), molecules. We report that most CO molecules are located within the hydrophobic core of LDs, whereas a small fraction (0.3−1.9 mol %) penetrates the monolayer. The solubility of CO in the phospholipid monolayer is relatively small. Due to a good miscibility with TO molecules, CO forms a liquid phase inside LD at 333 K. There is long-range order in the liquid TO−CO droplet core up to 8 nm from the phospholipid interface, resulting from the structuring of hydrophilic groups. This structuring slowly decays in the direction toward the LD center of mass. No sorting of TO and CO is detected, irrespective of the molar fractions simulated. The distribution of CO within the LDs is significant in determining the rate of their hydrolysis by surface-bound enzyme lipases, and thus has a subsequent impact on the levels of CO in plasma and LDLs.

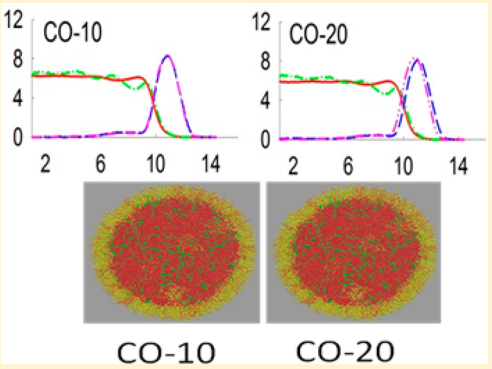

INTRODUCTION

Many efforts are now devoted in physical chemistry to studying molecular self-organization processes,[1,2] in particular, of lipid systems and lipid−water interfaces.[3,4] From a chemical perspective, cholesteryl esters (CEs) are lengthy, flexible molecules where a long fatty acid chain is linked to the hydroxyl group of cholesterol (CHOL)[5−9] via an ester, −COO−, bond. CEs are used by living cells to store and transport CHOL molecules in the form of lipid droplets (LDs)[10−12] throughout the body. Living systems mainly use linoleate and oleate fatty chains. Extracellular transport of CEs occurs by means of lipoprotein particles. Thus, CEs are strongly related to the development of atherosclerosis.[10,13] Consequently, metabolism of these molecules correlates closely with cardiovascular disease.

In both structure and storage functions, CEs are surrounded by amphiphilic phospholipid molecules. Due to such a structure, particles containing CEs become water friendly while possessing colloidal dimensions. Physical and chemical properties of cholesteryl esters and free CHOL are essentially different. The solubility of esters,[14,15] including cholesteryl esters, in the phospholipid monolayer is much smaller, as compared to the solubility of CHOL due to the absence of a polar hydroxyl group, OH.[16] However, it has been reported[17] that little amount of CEs solubilizes in the phospholipid monolayer, though CEs form separate phases in the presence of phospholipids. The actual amount of solubilized CEs depends on the composition of the phospholipid monolayer and the presence of the guest molecules. The availability of CEs at the lipid−water interfaces is crucial for the exchange and hydrolysis of CEs.[18] The latter is triggered by specific lipases. The cellular homeostasis of CEs thus depends on their distribution inside lipid droplets, which we aim to characterize in the current report.

A large number of experimental, computational, and theoretical studies demonstrated how the properties and water and aqueous ionic solutions alter in the vicinity of biological membranes.[19] In turn, properties of membranes and bilayers depend on the presence of aqueous solutions. Understanding these properties is important for research progress on many fronts. A comprehensive review of the existing computer simulations of bilayer-based systems was provided by Lyubartsev and Rabinovich.[20] Effects of lipid unsaturation, cholesterol presence, and the impact of other admixtures was discussed in great detail. However, lipid droplets are different from bilayers due to surface curvature and core composition. A comprehensive picture of the LD interface with water can be obtained through the analysis proposed by Jedlovszky and co-workers.[21] This methodology has been recently successfully applied to a variety of hydrophobe−water systems to characterize the orientation of the interfacial groups.[22−24]

Received: July 4, 2014
Revised: September 3, 2014
Published: September 4, 2014

   dx.doi.org/10.1021/jp506693d | *J. Phys. Chem. B* 2014, 118, 11145−11151

Table 1. List of the Simulated Systems[a]

system	N(TO)	N(CO)	N(POPC)	N(POPE)	N(water)	volume (nm^3)	time (μs)
CO-10	2000	222	1454	485	600 000	25 438	52.4
CO-20	2000	500	1521	507	600 000	25 856	49.6
CO-30	2000	857	1607	536	600 000	26 437	46.8
CO-40	2000	1333	1719	573	600 000	27 189	44.4
CO-50	2000	2000	1869	624	600 000	28 261	42.8

[a]The CO-*XX* systems represent lipid droplets in water. *XX* is the molar fraction (in %) of cholesteryl oleate in triolein. The amount of POPC and POPE molecules in each system was provided to cover the entire surface of the hydrophobic core.

Atomistic-resolution information concerning lipid droplets is scarce.[18] The diameter of small LDs is 20−50 nm.[10,13] The proximity of the dimensions to the diffraction limit causes significant problems to the experimental determination of LD structures and observation of their metabolism. Thermal fluctuations play an important role in the structure and dynamics of LDs. Often, only transient structures can be captured by the experimental techniques. Being liquid at living temperatures, LDs attain structures, which change over nanoseconds. Such fast dynamics poses an additional complexity to the experimental studies. Computer simulation methods, employing atomistic or coarse-grained molecular models, can circumvent the above-mentioned problems.[25] However, careful parametrization of potential energy functions is necessary to obtain reliable physical insights from the simulations.

This work describes coarse-grained molecular dynamics (MD) simulations of LDs composed of triolein (TO), cholesteryl oleate (CO), 1-palmitoyl-2-oleoylphosphatidylcholine (POPC), and 1-palmitoyl-2-oleoyl-*sn*-glycero-3-phosphoethanolamine (POPE) phospholipid molecules. The ratio between molar fractions of TO and CO was varied, providing five various compositions. The particular amounts of phospholipids were selected in order to provide full coverage of the lipid−water interface, while the molar ratio between POPC and POPE was kept at 3:1 in all systems. The total number of phospholipids was selected on the basis of the expected volume of the hydrophobic core and area per lipid (ca. 0.64 nm^2) determined in the bilayer systems. The sampling of each system has been done over 10 μs to obtain structure distribution functions.

SIMULATION DETAILS

The coarse-grained molecular dynamics simulation method within the MARTINI 2.1 framework[26] was used. Approximately every four neighboring heavy atoms were united to form a single spherical bead, which interacts with other beads via short-ranged Lennard-Jones (12,6) and Coulomb energy functions. The integrity of molecules is maintained by means of harmonic bond and angle potentials. The main acceleration experienced in coarse-grained simulations, as compared to conventional atomistic simulations, comes from a smaller number of interaction centers within a neighbor searching cutoff. The main disadvantage, in turn, is the inability of coarse-grained methodology to explicitly account for long-range interactions, which are often important in electrostatically driven hydrophilic systems.[27] The MARTINI force field (FF) was specifically tuned to reproduce physical chemical properties of the lipid systems. The FF was extensively validated in previous works.[26,28−30]

The list of the simulated systems and summarized MD simulation details are presented in Table 1. Figure 1 depicts snapshots of the selected simulated systems. All MD systems

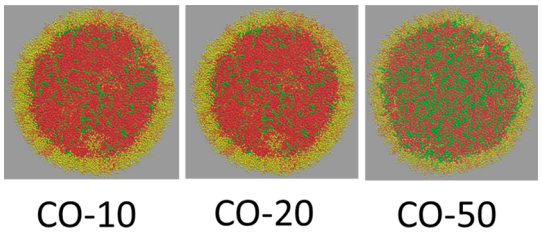

Figure 1. Final molecular configurations of the simulated MD systems. TO molecules are colored in red, CO molecules are colored in green, POPC molecules are colored in yellow, and POPE molecules are colored in orange. See Table 1 for the system designation.

were simulated over 40 μs to account for relatively slow conformational changes in lipid containing systems. The first 20 μs in all systems were disregarded as equilibration time. The statistical analysis was conducted using the remaining part of the trajectories. The mentioned times account for molecular dynamics acceleration due to coarse-graining (four times on average).

The MD trajectories were propagated using the GROMACS simulation suite.[31−33] The particle types defined in the MARTINI 2.1 coarse-grained force field[26,29] were used to construct all objects (POPC, POPE, TO, CO, and water) in all systems. All equilibrium simulations were conducted in the constant temperature constant pressure ensemble at 333 K and 1 bar using the classical Berendsen thermostat and barostat with relaxation times of 1.0 and 2.0 ps, respectively.[34] Though the Berendsen thermostat does not generate a correct canonical ensemble in the case of very small systems, for large systems, such as reported in the present work, the approximation yields roughly correct results for most calculated properties. The elevated temperature guarantees fast sampling and prevents the phenomenon of frozen MARTINI water.[30] Both electrostatic and Lennard-Jones (LJ) constituents of the potential were modified according to the shifted force scheme, with a shifted region from 0.0 to 1.2 nm for the Coulomb part and from 0.9 to 1.2 nm for the LJ part. The time-step for the integration of equations of motion was set to 0.02 ps. The time-step must be small enough to conserve total system energy upon molecular dynamics in the absence of temperature/pressure coupling. In the case of systems investigated in the present work, the integration time-step of 0.02 ps provides a perfect balance between fast molecular movements and reliable energy conservation. No intramolecular constraints, except those defined in the MARTINI 2.1 coarse-grained force field, were imposed. Conformational flexibility of biologically relevant molecules may play a key role in their structures and relaxation rates. The intermediate coordinates were saved every 5 ns for the calculation of ensemble-averaged properties.

The cluster analysis was performed using the single linkage approach. According to this approach, neighboring molecules

dx.doi.org/10.1021/jp506693d | J. Phys. Chem. B 2014, 118, 11145−11151

form a cluster when any bead belonging to a certain molecule is separated from any bead of a neighboring molecule by less than a cutoff distance. The cutoff distance (0.75 nm) was selected with respect to the size of beads of the MARTINI 2.1 coarse-grained force field.[26]

RESULTS AND DISCUSSION

Figure 1 depicts equilibrated configurations of LDs with higher and lower CO concentrations. The snapshots were taken at the end of MD simulations. Therefore, they correspond to the local free energy minima of the corresponding systems at 333 K. The hydrophobic core of the LD in the case of the CO-poor system is formed by TO molecules with a certain presence of CO. In turn, the core of the CO-rich system is implemented by a mixture of CO and TO. Both visual examination of molecular snapshots and basic cluster search indicate a perfect miscibility of the two liquids, which both belong to the class of esters. The amphiphilic monolayer composed of POPC (75 mol %) and POPE (25 mol %) decreases the surface tension of the droplets and makes them water-soluble.[10,17] The LDs, therefore, form a genuine colloid system in aqueous media. The solubility of TO in the monolayer is rather low, in good agreement with experimental data. Thermal motion, expectedly, plays a significant role in the diffusion of TO and CO molecules close to the lipid−water interface.

Interestingly, a certain amount of phospholipids (both POPC and POPE, irrespective of identity) was recorded in the hydrophobic core while far from the lipid−water interface. Note that at the beginning of the simulations all POPC and POPE molecules were deliberately placed so that their head groups were in direct contact with water beads. The amount of phospholipids was calculated on the basis of the tentative volume of the hydrophobic core. The latter was, in turn, estimated on the basis of the expected density of TO and CO binary mixtures. As it is impossible to predict the exact density of the nonideal binary mixture on the basis of only the densities of pure constituents, it is also impossible to rigorously estimate the number of phospholipids in the monolayer.

The fact that a certain amount of phospholipids migrates into the LD core suggests that tight competition among phospholipids takes place at the interface. The phospholipids, which cannot stabilize at the interface, generate small (less than 10 molecules) inverted micelles. The estimation is based on the visual examination of numerous simulation snapshots in combination with radial distribution functions. These micelles penetrate the hydrophobic core. An alternative process would include separation of direct micelles into an aqueous phase. However, we did not observe this process in any simulated system. We hypothesize that inverted micelles in the lipid core are more energetically favorable than free micelles in the aqueous phase, provided that an excess amount of the phospholipid molecules was supplied. However, specific free energy calculations are necessary to derive a quantitative conclusion. The existence of a limited amount of inverted phospholipid micelles in the LD core has never been reported before. The experimental information is also lacking regarding how many phospholipid molecules normally belong to LDs in a living body as a function of LD surface area. The available experimental information contains w/w percentages of lipids and proteins in various kinds of intracellular lipid particles.[35]

Figure 2 depicts the radius of gyration of the whole droplet (TO, CO, POPC, POPE) compared with the radius of gyration of the hydrophobic part (TO, CO) only. The thermodynamic

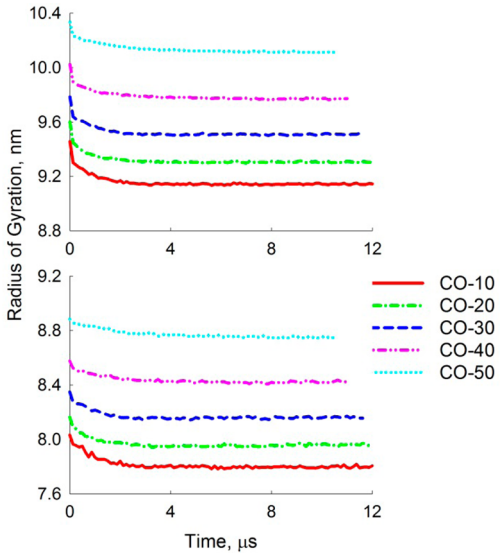

Figure 2. (top) Radius of gyration of the entire LD. (bottom) Radius of gyration of the hydrophobic part (TO and CO molecules only) of the LD. Radius of gyration is an important measure of structural equilibration of the simulated system.

equilibration takes quite a significant amount of time, over 2 μs, in the case of all systems. This fact well justifies the necessity of the current large-scale simulations. The fact is also in reasonable agreement with a modern understanding of time-scales of lipid dynamics. The radius of gyration is in direct proportion to the total number of lipids in the corresponding system (Table 1). The simulated radii correspond to the size of the smallest experimentally observed lipid droplets.

Figure 3 depicts the radial density of all beads belonging to lipids versus their distance from the LD center of mass. Note

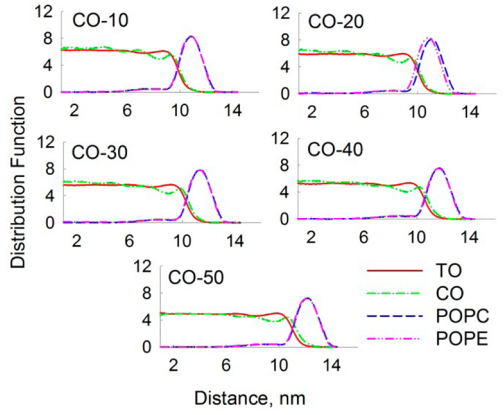

Figure 3. Radial distribution of the number density of TO, CO, POPC, and POPE molecules as a function of the distance from the LD center of mass. See text for the definition of this function.

that the LD center of mass was updated at every calculation time-step. The distribution function was defined to be consistent with the conventional radial distribution function. That is, the value of this function at every point shows by how many times the number density of a certain lipid exceeds the average number density of this same lipid in the simulated MD box. Using this knowledge, number or mass densities of molecules can be recovered, where necessary. In CO-poor systems, the corresponding density fluctuates more significantly

dx.doi.org/10.1021/jp506693d | J. Phys. Chem. B 2014, 118, 11145−11151

than in the systems containing more CO. This can be explained by less comprehensive statistics in the case of a relatively small amount of CO molecules, while the sampling time to represent a statistical ensemble is sufficient. Distribution functions confirm visual observation. Indeed, the lipid–water interface is, at all times, occupied by the phospholipid monolayer. The fact that namely a monolayer, as opposed to different kinds of multilayer lipid structures, is formed is suggested by the width of the Gaussian-like density distribution. Interestingly, there is no qualitative difference between POPC and POPE. In turn, Figure 1 suggests that these phospholipids are evenly distributed across the monolayer without formation of any detectable molecular aggregates. Note that the coarse-grained force field[26] was employed to describe the systems. Although this force field was extensively validated versus a few key properties of lipids and other biological molecules,[26,36−39] its accuracy and precision might not be enough to capture a fine difference between POPC and POPE in the studied systems. Recall that POPC and POPE differ slightly by only one bead representing a headgroup (choline, ethanolamine). We propose that the observation about too little difference between POPC and POPE concerning their location in the LD monolayer is taken with caution.

TO and CO lipids are uniformly distributed in the hydrophobic core. This indicates their excellent miscibility with one another. Note that both TO and CO intersect the curves of phospholipid density. This indicates a certain solubility of TO and CO lipids in the POPC/POPE monolayer. The biological mission of LDs is to transfer cholesteryl esters which are finally decomposed providing CHOL and fatty acids. The lipid hydrolysis is catalyzed by lipase enzymes located at the lipid–water interface. It is important that the lipase can, first of all spatially, access cholesteryl esters to initiate lipolysis. Consequently, it is important that CO is present close to the interface, as suggested by our simulations. Once the initial amount of CO at the lipid–water interface has reacted, additional esters arrive from inside to satisfy the solubility limit. Current information on lipid droplet breakdown, known as lipolysis, has been derived from the studies in adipocytes. Fatty acids are released from cells as fuel for tissues. The sequential hydrolysis of triacylglycerols is catalyzed by the sequential action of three lipases. An availability of esters to lipases depends on TO and CO structure in the vicinity of the lipid–water interface.

An interesting feature is a decreased density of CO molecules near the monolayer. TO molecules do not exhibit such a density decrease. There is a possibility that a certain long-range structure is present within the lipid medium. If such a structure does exist, it must be maintained through stronger electrostatic attraction between the polar groups. In order to corroborate this speculation, we plot the densities of polar and nonpolar groups of all lipids (Figure 4). Indeed, long-range structure is observed, starting at the lipid–water interface. Density fluctuations attenuate after 8 nm from the interface. No long-range structure is present for nonpolar (hydrophobic) beads.

Another important question is whether weakly polar ester groups of CO and TO form any sort of long-range structure in the essentially nonpolar LD core. Figure 5 suggests that ester groups, which belong to TO (three groups per molecule), produce such a structure, whereas the structure is very weak in the case of CO (one group per molecule). The period of density oscillations, ca. 3 nm, roughly corresponds to the linear dimensions of the TO molecule in various conformations. The

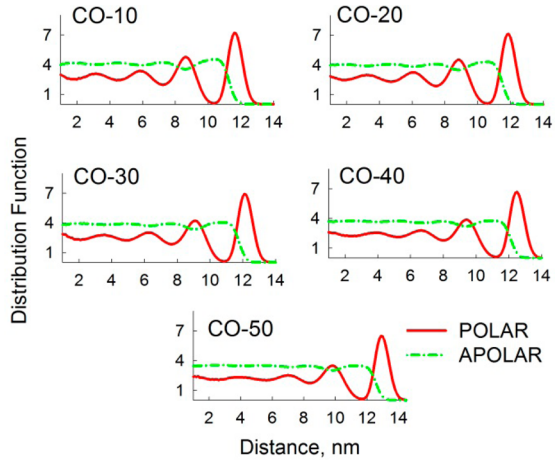

Figure 4. Radial distribution of the number density of polar (PO_4, NC_3, NH_3, COO beads) and nonpolar (all beads exhibiting a lower hydrophilicity than the COO ester group) moieties in all simulated lipid molecules as a function of the distance from the LD center of mass.

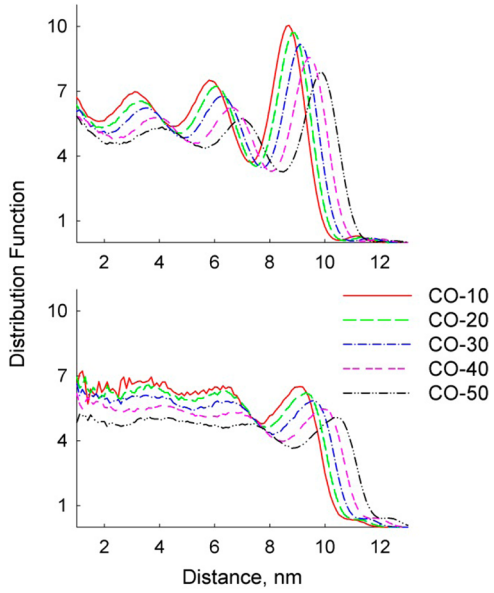

Figure 5. Probability of location of ester, COO groups of TO (top) and CO (bottom) vs the distance from the LD center of mass. The center of mass was computed on the basis of the positions of all lipid molecules, including phospholipids.

structure is most clearly seen in the TO-rich systems and gradually vanishes as the CO content increases. Therefore, the number of polar beads per molecule (density of polar beads in the LD core) may determine the ability of an ester molecule to exhibit a long-range structure. The density of polar beads in CO is smaller than that in TO; compare 1/8 vs 3/18. Although a coarse-grained representation does not account for long-range interactions explicitly, it can reproduce these interactions implicitly thanks to specifically tuning short-range potential functions. Therefore, the reported results are deemed reliable and force field independent.

The distribution of CO in the LD is determined by its excellent miscibility with TO. In CO-rich systems, CO forms a single large cluster, although it is evenly spread in the TO medium. The cluster formation occurs, therefore, due to purely

dx.doi.org/10.1021/jp506693d | J. Phys. Chem. B 2014, 118, 11145−11151

steric reasons. Figure 6 summarizes the probability of small cluster formation (up to 7 CO molecules per cluster). The

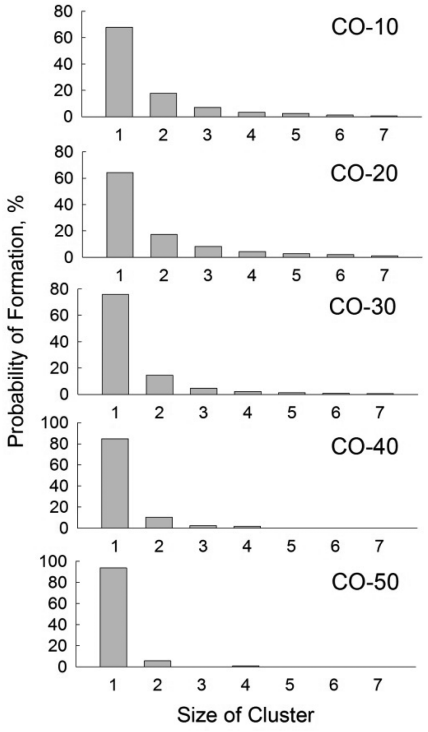

Figure 6. Fractions of small CO clusters in LDs of various compositions.

largest fraction (over 80%) of CO, which does not belong to a single large cluster, exists as monomers. Twenty mol % of CO form dimers. The fraction of dimers decreases as the CO content increases. Trimers and larger CO clusters are formed with even lower probability. To recapitulate, CO in LD does not exhibit a tendency for aggregation based on any specific nonbonded interactions. It exists as a weakly structured liquid phase, in compliance with Figure 5.

The thickness of the phospholipid monolayer, covering the LD (Figure 1), can be derived from the distributions of number densities of head and tail beads of phospholipids, as shown in Figure 7. In the case of complete coverage of the LD surface by phospholipids, the monolayer thickness constitutes a well-defined quantity. It can be compared to the thickness of a bilayer formed by the same phospholipid composition. Figure 8 depicts the radius of LD with a monolayer and the radius of LD without a monolayer. Note that calculations were performed using the same MD systems, but the coordinates of phospholipids were disregarded to obtain the radius of the uncovered droplet.

On the basis of the calculated thickness of the monolayers (2.2 nm), one can conclude that phospholipids "stand straight" in the monolayer in order to maximize the separation between water and ester molecules. Provided that the amount of phospholipids is not sufficient, alternative orientations may be observed. The density peaks, corresponding to the head groups of POPC and POPE, are smeared in a similar way as the peaks corresponding to the phospholipid tails. This suggests that the monolayer exhibits significant mobility. Despite the reported long-range structure, the monolayer remains in the liquid phase. Solubilities of TO and CO molecules in the monolayer

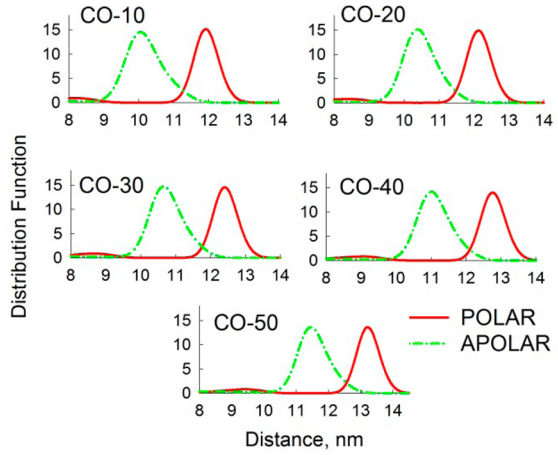

Figure 7. Radial distributions of the number density of the phospholipid headgroup (NC_3, NH_3) and tail (C_xH_y) as a function of the distance from the LD center of mass.

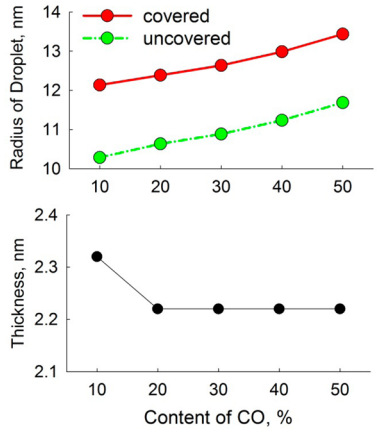

Figure 8. (top) Radius of the entire LD ("covered" by the phospholipid monolayer, red solid line) and radius of the hydrophobic core of LD ("uncovered" LD, green dash-dotted line). (bottom) Thickness of the monolayer formed by phospholipid (POPC and POPE) molecules at the surface of the LD. Note that the uncertainty of the presented numbers is determined by the half of a bead diameter (ca. 0.3 nm).

can be reconstructed from the corresponding number density distributions (Figure 3). These solubilities can be compared to solubilities of TO and CO molecules in the phospholipid bilayer.[14,15] However, it would be more correct to refer to partitioning between the ester phase and monolayer, because neither TO nor CO are restrained in the monolayer. If the solubility limit in the monolayer is reached, the excess ester molecules would rather migrate to the ester phase than create a phase within the monolayer. The computed content of TO in the phospholipid monolayer ranges from 1.7 mol % in the CO-10 system to 0.6 mol % in the CO-50 system; i.e., the increase of CO content leads to a decrease of the TO presence in the monolayer. In turn, the CO content in the monolayer increases from 0.3 mol % (CO-10) to 1.9 mol % (CO-50). This trend can be explained by availability of esters, since any specific affinity of TO or CO toward the simulated phospholipids is unlikely. If the comparison of solubility is done in terms of molar fractions, CO solubility is higher than TO solubility. However, the mass and volume of CO are smaller than those of TO. Therefore, the difference in solubility diminishes if a

dx.doi.org/10.1021/jp506693d | J. Phys. Chem. B 2014, 118, 11145−11151

comparison is done in mass or volume percent. The total solubility of esters in the monolayer (TO+CO in POPC +POPE) does not exhibit any dependence on the ester ratio and fluctuates around 2 mol %.

SAMPLING ISSUES

Sampling of lipid containing systems is a key issue, since these systems exhibit high shear viscosity and small self-diffusion coefficients of the components. In order to rely on the simulation results, ergodicity of the MD simulation should be ensured; i.e., an average over the sampled time region should be equal to an average over the sampled spatial region. After location of the free energy minimum, the system must visit most states of the phase space at a given temperature and pressure. The coarse-grained models possess an advantage over all-atom force field models in the context of proper sampling of phase space. The process of coarse-graining is a substitution of atoms by larger-size beads, resulting in the decrease of total degrees of freedom per system. The reduction of degrees of freedom means a simpler potential energy surface, which must be sampled during molecular dynamics. Therefore, in addition to a possibility of using a larger integration time-step, the coarse-grained representations accelerate a sampling speed. Diffusion constants can be directly retrieved from the MD trajectory. As such, they constitute an important measure of how well the simulated time corresponds to the simulated energy surface. The average diffusion coefficient for all lipid molecules in the investigated systems is equal to ca. 1×10^{-10} m^2 s^{-1} (at 333 K). On the basis of this diffusion constant, one easily estimates that an average lipid molecule diffuses by slightly more than 10 nm during the course of the MD simulation. This distance is comparable to the radius of each LD. This fact provides solid evidence, although not a rigorous proof, for proper sampling. The above estimate does not account for symmetry considerations, which will further decrease minimum necessary sampling times, as all TO and CO molecules in the core are physically identical and most phospholipid molecules do not (and should not) diffuse to the interior of the droplet. Note that the reported self-diffusion coefficient is provided for information on the apparent dynamics of the simulated systems. It should be compared to experimental values or to diffusion coefficients derived from all-atomistic molecular dynamics studies very carefully.

CONCLUSIONS

Physical chemistry of lipid droplets is an emerging research area inspired by their relation to common diseases and fat metabolism.[10,12,13,40] These nanoscale and microscale structures are dedicated to CHOL storage and transfer throughout the living body. Most CHOL is stored in the form of cholesteryl esters, such as CO. Once necessity arises, an enzymatic reaction takes place to release CHOL. This computational investigation presents a molecular dynamics investigation of LD structure as a function of CO content. Free CHOL was omitted in the simulations for clarity, because CHOL content is often marginal as compared to the content of esterified CHOL. Our simulations predict that TO and CO maintain a single phase, which constitutes a hydrophobic core of LD. However, there is clear long-range order in the droplet core. A certain amount of esters is dissolved in the phospholipid monolayer. In turn, an excess of POPC and POPE phospholipids migrate from the interface to the LD core creating inverted micelles. The reported results should promote a molecular-level understanding[10,12,40] of the structure and processes occurring in lipid droplets, low-density lipoprotein particles, and colloid systems possessing lipid–water interfaces.[3]

AUTHOR INFORMATION

Corresponding Authors

*E-mail: vvchaban@gmail.com; chaban@sdu.dk.
*E-mail: hkhandel@sdu.dk.

Notes

The authors declare no competing financial interest.

ACKNOWLEDGMENTS

The discussed computations have been partially carried out at the SDU node of the Danish Center for Scientific Computing. We acknowledge that part of the results of this research have been achieved using the PRACE-2IP project (FP7 RI-283493) resource Archer based in Great Britain. This research has been funded by a Lundbeckfonden Young Investigator Grant (Khandelia).

REFERENCES

(1) Contal, E.; Morere, A.; Thauvin, C.; Perino, A.; Meunier, S.; Mioskowski, C.; Wagner, A. Photopolymerized Lipids Self-Assembly for the Solubilization of Carbon Nanotubes. *J. Phys. Chem. B* **2010**, *114*, 5718–5722.
(2) Colherinhas, G.; Fileti, E. Molecular Description of Surfactant-Like Peptide Based Membranes. *J. Phys. Chem. C* **2014**, *118*, 9598–9603.
(3) Staples, E.; Penfold, J.; Tucker, I. Adsorption of Mixed Surfactants at the Oil-Water Interface. *J. Phys. Chem. B* **2000**, *104*, 606–614.
(4) Vazdar, M.; Wernersson, E.; Khabiri, M.; Cwiklik, L.; Jurkiewicz, P.; Hof, M.; Mann, E.; Kolusheva, S.; Jelinek, R.; Jungwirth, P. Aggregation of Oligoarginines at Phospholipid Membranes: Molecular Dynamics Simulations, Time-Dependent Fluorescence Shift, and Biomimetic Colorimetric Assays. *J. Phys. Chem. B* **2013**, *117*, 11530–11540.
(5) Venkatatraman, N. V.; Vasudevan, S. Cholesterol Binding to the Alkyl Chains of an Intercalated Surfactant Bilayer. *J. Phys. Chem. B* **2003**, *107*, 10119–10126.
(6) Jurak, M. Thermodynamic Aspects of Cholesterol Effect on Properties of Phospholipid Monolayers: Langmuir and Langmuir-Blodgett Monolayer Study. *J. Phys. Chem. B* **2013**, *117*, 3496–3502.
(7) Sengupta, D. Cholesterol Modulates the Structure, Binding Modes, and Energetics of Caveolin-Membrane Interactions. *J. Phys. Chem. B* **2012**, *116*, 14556–14564.
(8) O'Connor, J. W.; Klauda, J. B. Lipid Membranes with a Majority of Cholesterol: Applications to the Ocular Lens and Aquaporin 0. *J. Phys. Chem. B* **2011**, *115*, 6455–6464.
(9) Plesnar, E.; Subczynski, W. K.; Pasenkiewicz-Gierula, M. Comparative Computer Simulation Study of Cholesterol in Hydrated Unary and Binary Lipid Bilayers and in an Anhydrous Crystal. *J. Phys. Chem. B* **2013**, *117*, 8758–8769.
(10) Ohsaki, Y.; Suzuki, M.; Fujimoto, T. Open Questions in Lipid Droplet Biology. *Chem. Biol.* **2014**, *21*, 86–96.
(11) Fujimoto, T.; Ohsaki, Y.; Cheng, J.; Suzuki, M.; Shinohara, Y. Lipid Droplets: A Classic Organelle with New Outfits. *Histochem. Cell Biol.* **2008**, *130*, 263–279.
(12) Beckman, M. Cell Biology - Great Balls of Fat. *Science* **2006**, *311*, 1232–1234.
(13) Salo, V. T.; Ohsaki, Y.; Ikonen, E. Lipid Droplet Biogenesis: When the Endoplasmic Reticulum Starts to Fatten Up. *Curr. Opin. Lipidol.* **2011**, *22*, 505–506.

(14) Spooner, P. J. R.; Small, D. M. The Effect of Free-Cholesterol on the Solubility of Triolein in Phospholipid-Bilayers. *Biophys. J.* **1987**, *51*, A188−A188.
(15) Spooner, P. J. R.; Small, D. M. Effect of Free-Cholesterol on Incorporation of Triolein in Phospholipid-Bilayers. *Biochemistry* **1987**, *26*, 5820−5825.
(16) Spooner, P. J. R.; Hamilton, J. A.; Gantz, D. L.; Small, D. M. The Effect of Free-Cholesterol on the Solubilization of Cholesteryl Oleate in Phosphatidylcholine Bilayers - a C-13-Nmr Study. *Biochim. Biophys. Acta* **1986**, *860*, 345−353.
(17) Tauchi-Sato, K.; Ozeki, S.; Houjou, T.; Taguchi, R.; Fujimoto, T. The Surface of Lipid Droplets Is a Phospholipid Monolayer with a Unique Fatty Acid Composition. *J. Biol. Chem.* **2002**, *277*, 44507−44512.
(18) Koivuniemi, A.; Heikela, M.; Kovanen, P. T.; Vattulainen, I.; Hyvonen, M. T. Atomistic Simulations of Phosphatidylcholines and Cholesteryl Esters in High-Density Lipoprotein-Sized Lipid Droplet and Trilayer: Clues to Cholesteryl Ester Transport and Storage. *Biophys. J.* **2009**, *96*, 4099−4108.
(19) Berkowitz, M. L.; Vacha, R. Aqueous Solutions at the Interface with Phospholipid Bilayers. *Acc. Chem. Res.* **2012**, *45*, 74−82.
(20) Lyubartsev, A. P.; Rabinovich, A. L. Recent Development in Computer Simulations of Lipid Bilayers. *Soft Matter* **2011**, *7*, 25−39.
(21) Jedlovszky, P.; Vincze, A.; Horvai, G. New Insight into the Orientational Order of Water Molecules at the Water/1,2-Dichloroethane Interface: A Monte Carlo Simulation Study. *J. Chem. Phys.* **2002**, *117*, 2271−2280.
(22) Jorge, M.; Cordeiro, M. N. D. S. Intrinsic Structure and Dynamics of the Water/Nitrobenzene Interface. *J. Phys. Chem. C* **2007**, *111*, 17612−17626.
(23) Benkova, Z.; Cordeiro, M. N. D. S. Molecular Dynamics Study of Water Interacting with Siloxane Surface Modified by Poly(Ethylene Oxide) Chains. *J. Phys. Chem. C* **2011**, *115*, 18740−18751.
(24) Hantal, G.; Voroshylova, I.; Cordeiro, M. N. D. S.; Jorge, M. A Systematic Molecular Simulation Study of Ionic Liquid Surfaces Using Intrinsic Analysis Methods. *Phys. Chem. Chem. Phys.* **2012**, *14*, 5200−5213.
(25) Khandelia, H.; Duelund, L.; Pakkanen, K. I.; Ipsen, J. H., Triglyceride Blisters in Lipid Bilayers: Implications for Lipid Droplet Biogenesis and the Mobile Lipid Signal in Cancer Cell Membranes. *PLoS One* **2010**, *5*.
(26) Marrink, S. J.; Risselada, H. J.; Yefimov, S.; Tieleman, D. P.; de Vries, A. H. The Martini Force Field: Coarse Grained Model for Biomolecular Simulations. *J. Phys. Chem. B* **2007**, *111*, 7812−7824.
(27) Anezo, C.; de Vries, A. H.; Holtje, H. D.; Tieleman, D. P.; Marrink, S. J. Methodological Issues in Lipid Bilayer Simulations. *J. Phys. Chem. B* **2003**, *107*, 9424−9433.
(28) Wassenaar, T. A.; Ingolfsson, H. I.; Priess, M.; Marrink, S. J.; Schafer, L. V. Mixing Martini: Electrostatic Coupling in Hybrid Atomistic-Coarse-Grained Biomolecular Simulations. *J. Phys. Chem. B* **2013**, *117*, 3516−3530.
(29) de Jong, D. H.; Singh, G.; Bennett, W. F. D.; Arnarez, C.; Wassenaar, T. A.; Schafer, L. V.; Periole, X.; Tieleman, D. P.; Marrink, S. J. Improved Parameters for the Martini Coarse-Grained Protein Force Field. *J. Chem. Theory Comput.* **2013**, *9*, 687−697.
(30) Yesylevskyy, S. O.; Schafer, L. V.; Sengupta, D.; Marrink, S. J. Polarizable Water Model for the Coarse-Grained Martini Force Field. *PLoS Comput. Biol.* **2010**, *6*, e1000810.
(31) Van der Spoel, D.; Lindahl, E.; Hess, B.; Groenhof, G.; Mark, A. E.; Berendsen, H. J. C. Gromacs: Fast, Flexible, and Free. *J. Comput. Chem.* **2005**, *26*, 1701−1718.
(32) Hess, B.; Kutzner, C.; van der Spoel, D.; Lindahl, E. Gromacs 4: Algorithms for Highly Efficient, Load-Balanced, and Scalable Molecular Simulation. *J. Chem. Theory Comput.* **2008**, *4*, 435−447.
(33) Lindahl, E.; Hess, B.; van der Spoel, D. Gromacs 3.0: A Package for Molecular Simulation and Trajectory Analysis. *J. Mol. Model.* **2001**, *7*, 306−317.
(34) Berendsen, H. J. C.; Postma, J. P. M.; Vangunsteren, W. F.; Dinola, A.; Haak, J. R. Molecular-Dynamics with Coupling to an External Bath. *J. Chem. Phys.* **1984**, *81*, 3684−3690.
(35) Zweytick, D.; Athenstaedt, K.; Daum, G. Intracellular Lipid Particles of Eukaryotic Cells. *Biochim. Biophys. Acta, Rev. Biomembr.* **2000**, *1469*, 101−120.
(36) Marrink, S. J.; Tieleman, D. P. Perspective on the Martini Model. *Chem. Soc. Rev.* **2013**, *42*, 6801−6822.
(37) Apajalahti, T.; Niemela, P.; Govindan, P. N.; Miettinen, M. S.; Salonen, E.; Marrink, S. J.; Vattulainen, I. Concerted Diffusion of Lipids in Raft-Like Membranes. *Faraday Discuss.* **2010**, *144*, 411−430.
(38) Lee, H.; de Vries, A. H.; Marrink, S. J.; Pastor, R. W. A Coarse-Grained Model for Polyethylene Oxide and Polyethylene Glycol: Conformation and Hydrodynamics. *J. Phys. Chem. B* **2009**, *113*, 13186−13194.
(39) Hinner, M. J.; Marrink, S. J.; de Vries, A. H. Location, Tilt, and Binding: A Molecular Dynamics Study of Voltage-Sensitive Dyes in Biomembranes. *J. Phys. Chem. B* **2009**, *113*, 15807−15819.
(40) Sturley, S. L.; Hussain, M. M. Thematic Review Series: Lipid Droplet Synthesis and Metabolism: From Yeast to Man Lipid Droplet Formation on Opposing Sides of the Endoplasmic Reticulum. *J. Lipid Res.* **2012**, *53*, 1800−1810.